

Numerical analysis of a singularly perturbed 4th order problem with a shift term

Sebastian Franz*, Kleio Liotati†

September 22, 2023

Abstract

We consider a one-dimensional singularly perturbed 4th order problem with the additional feature of a shift term. An expansion into a smooth term, boundary layers and an inner layer yields a formal solution decomposition, and together with a stability result we have estimates for the subsequent numerical analysis. With classical layer adapted meshes we present a numerical method, that achieves supercloseness and optimal convergence orders in the associated energy norm. We also consider coarser meshes in view of the weak layers. Some numerical examples conclude the paper and support the theory.

AMS subject classification (2010): 65L11, 65L60

Key words: singularly perturbed, 4th order problem, shift, solution decomposition, mesh generation

1 Introduction

In this paper we consider for $m \in \{1, 2\}$ the singularly perturbed 4th order problem

$$Lu(x) := \varepsilon^2 u^{(4)}(x) - b(x)u''(x) + c(x)u(x) + d(x)u(x-1) = f(x), \quad x \in \Omega = (0, 2), \quad (1a)$$

$$u(x) = \Phi(x), \quad x \in (-1, 0), \quad (1b)$$

$$u(0) = u(2) = 0, \quad (1c)$$

$$u^{(m)}(0) = u^{(m)}(2) = 0, \quad (1d)$$

where Φ is a given function with $\Phi(0) = u(0) = 0$ and $\Phi^{(m)}(0) = u^{(m)}(0) = 0$, which is not a practical restriction, and b, c, d are smooth functions with $b \geq \beta^2 > 0$ and $c - \frac{\|d\|_{L^\infty(1,2)}}{2} - \frac{\|b'\|_{L^\infty}^2}{2\beta^2} \geq \delta > 0$. The case $m = 1$ in (1d) can be seen as modelling a clamped 1d beam, while $m = 2$ models a supported 1d beam.

*Institute of Scientific Computing, Technische Universität Dresden, Germany. e-mail: sebastian.franz@tu-dresden.de

†Technische Universität Dresden, Germany. e-mail: klio9965@gmail.com

For second-order singularly perturbed problems with a shift (sometimes also called a delay) we find some papers on numerical analysis in the literature, see e.g. [1, 2, 4, 6–8, 11] for the reaction-diffusion case and [3, 12, 16, 17] for the convection-diffusion case. For the fourth order problem this is the first paper on problems with a shift.

We will follow the classical way of analysing numerical methods for singularly perturbed problems, see also [14]. To do this, we first provide a solution decomposition of our problem. One way to do this is to make assumptions about the signs of the coefficients and derive a maximum principle. We proceed in another way, without restricting the coefficients, and use a stability result involving Green's function estimates, see Section 2 and the appendix. Once the structure of the solution is known, the construction of layer-adapted meshes is straightforward, see Section 3. But we will also look at another construction, a more problem-orientated one in Section 5. Section 4 contains the numerical analysis on the standard layer-adapted meshes. Finally, there are numerical examples in Section 6, which provide some numbers to support the theoretical claims.

Notation: We will denote by $L^p(D)$ the classical Lebesgue norm over the domain D and skip the reference to the domain when $D = \Omega$.

2 Solution decomposition

We give a derivation of a formal solution decomposition for the solution u of (1) in the case of constant coefficients b and c , but assume that it also holds for the case of variable coefficients. In the following we set $m = 1$, but the derivation can easily be adapted to the other case.

As a first step, we rewrite our problem (1) by splitting Ω at $x = 1$. For $u = u_1\chi_{[0,1)} + u_2\chi_{[1,2]}$ we get

$$\varepsilon^2 u_1^{(4)}(x) - b(x)u_1''(x) + c(x)u_1(x) = f(x) - d(x)\Phi(x-1), \quad x \in (0, 1), \quad (2a)$$

$$\varepsilon^2 u_2^{(4)}(x) - b(x)u_2''(x) + c(x)u_2(x) = f(x) - d(x)u_1(x-1), \quad x \in (1, 2), \quad (2b)$$

$$u_1(0) = u_2(2) = 0, \quad (2c)$$

$$u_1'(0) = u_2'(2) = 0, \quad (2d)$$

$$\llbracket u \rrbracket(1) = \llbracket u' \rrbracket(1) = \llbracket u'' \rrbracket(1) = \llbracket u''' \rrbracket(1) = 0, \quad (2e)$$

where $\llbracket v \rrbracket(1) := v_2(1^+) - v_1(1^-)$ denotes the jump of v at $x = 1$. In addition to the original conditions, we have the continuity conditions (2e). Together with the differential equations (2a) and (2b) they give $u \in C^4(\Omega)$ if $f \in C(\Omega)$.

To derive the formal decomposition, we need some auxiliary problems. For the so-called outer expansion, we replace u by

$$\sum_{k=0}^{\infty} \varepsilon^k S_k(x) := \sum_{k=0}^{\infty} \varepsilon^k (S_{k,left}(x)\chi_{(0,1)}(x) + S_{k,right}(x)\chi_{(1,2)}(x))$$

in (2). Comparing the lowest order power of ε we get for S_0 from the system

$$\begin{aligned} -bS_{0,left}''(x) + cS_{0,left}(x) &= f(x) - d\Phi(x-1), \quad x \in \Omega = (0, 1), \\ -bS_{0,right}''(x) + cS_{0,right}(x) &= f(x) - dS_{0,left}(x-1), \quad x \in \Omega = (1, 2), \\ S_{0,left}(0) &= S_{0,right}(2) = 0, \\ \llbracket S_0 \rrbracket(1) &= 0, \llbracket S_0' \rrbracket(1) = 0. \end{aligned}$$

Its solution holds $S_0 \in C^2(\Omega) \setminus C^3(\Omega)$ if $f \in C(\Omega)$ and it does not satisfy the second set of boundary conditions. So we use inner expansions to correct the boundary values and the regularity problem. For the left boundary we use a scaled variable $\xi = x/\varepsilon$, replace u in (2) by

$$\sum_{k=1}^{\infty} \varepsilon^k E_{k,left}(x) := \sum_{k=1}^{\infty} \varepsilon^k \tilde{E}_{k,left}(\xi)$$

and include the boundary condition correction. At the lowest level of ε this is

$$\begin{aligned} \tilde{E}_{1,left}^{(4)}(\xi) - b\tilde{E}_{1,left}''(\xi) &= 0, \\ \tilde{E}_{1,left}'(0) &= -S_0'(0). \end{aligned}$$

To get a unique solution, we assume that $\tilde{E}_{1,left}$ is exponentially decaying. As a result, the boundary condition for the derivative is satisfied, but we introduce a discrepancy in the first boundary condition:

$$(S_0 + \varepsilon E_{1,left})(0) = \varepsilon E_{1,left}(0) = \mathcal{O}(\varepsilon).$$

We will deal with this in the next step of our expansion. Using $\eta = (2-x)/\varepsilon$ and $E_{k,right}(x) = \tilde{E}_{k,right}(\eta)$ we can apply the same idea to correct the boundary value at $x = 2$.

To resolve the regularity issue at $x = 1$, we introduce two inner expansions. With the two scaled variables $\psi = (1-x)/\varepsilon = \eta - 1/\varepsilon$ and $\theta = (x-1)/\varepsilon = \xi - 1/\varepsilon$ we replace u in (2) by

$$\sum_{k=3}^{\infty} \varepsilon^k W_k(x) = \sum_{k=3}^{\infty} \varepsilon^k (\tilde{W}_{k,left}(\psi)\chi_{(0,1)}(x) + \tilde{W}_{k,right}(\theta)\chi_{(1,2)}(x)).$$

The lowest order of ε now gives the following coupled problem

$$\begin{aligned} \tilde{W}_{3,left}^{(4)}(\psi) - b\tilde{W}_{3,left}''(\psi) &= -d\tilde{E}_{1,right}(\psi), \\ \tilde{W}_{3,right}^{(4)}(\theta) - b\tilde{W}_{3,right}''(\theta) &= -d\tilde{E}_{1,left}(\theta), \\ \tilde{W}_{3,left}''(0) &= \tilde{W}_{3,right}''(0), \\ -\tilde{W}_{3,left}'''(0) &= \tilde{W}_{3,right}'''(0) - \llbracket S_0''' \rrbracket(1), \end{aligned}$$

where we have included the correction in the second continuity condition. We have also included as right-hand sides the shifted terms resulting from the boundary corrections,

which were not treated before. Note that W_3 and its first derivative are not continuous at $x = 1$. Let

$$V_0 := S_0 + \varepsilon(E_{1,left} + E_{1,right}) + \varepsilon^3 W_3$$

be the sum of the components derived so far. Then, we have

$$\begin{aligned} \llbracket V_0'' \rrbracket(1) = \llbracket V_0''' \rrbracket(1) = 0, \quad \llbracket V_0 \rrbracket(1) = \varepsilon^3 \llbracket W_3 \rrbracket(1) = \mathcal{O}(\varepsilon^3), \quad \llbracket V_0' \rrbracket(1) = \varepsilon^3 \llbracket W_3' \rrbracket(1) = \mathcal{O}(\varepsilon^2), \\ V_0(0) = \varepsilon E_{1,left}(0) + \mathcal{O}\left(e^{-\frac{\beta}{\varepsilon}}\right), \quad V_0'(0) = \mathcal{O}\left(e^{-\frac{\beta}{\varepsilon}}\right), \\ V_0(2) = \varepsilon E_{1,right}(2) + \mathcal{O}\left(e^{-\frac{\beta}{\varepsilon}}\right), \quad V_0'(2) = \mathcal{O}\left(e^{-\frac{\beta}{\varepsilon}}\right). \end{aligned}$$

The remaining jumps and $\mathcal{O}(\varepsilon)$ -violations of the boundary conditions can all be incorporated into the S -problems of the next steps in the expansion. In addition, let us look at the residual, the terms so far not included into our differential problems. They are

$$\varepsilon^2 S_0^{(4)} + \varepsilon c(E_{1,left} + E_{1,right}) + \varepsilon^3 cW_3 + \varepsilon^3 dW_{3,left}(\cdot - 1).$$

The first can be included as the right-hand side in the problem for $\varepsilon^2 S_2$, the next two in the problems for $\varepsilon^3 E_3$ and the third one in the problem for $\varepsilon^5 W_5$. Note that these are the components of V_2 with

$$V_k := \varepsilon^k S_k + \varepsilon^{k+1}(E_{k+1,left} + E_{k+1,right}) + \varepsilon^{k+3} W_{k+3}.$$

The last term with the shift-operator can be included in the right-hand side of the problem for $\varepsilon^5 E_{5,right}$.

In general, we have the following sub-problems. For $k \geq 0$ the outer expansion solves

$$-bS_{k,left}''(x) + cS_{k,left}(x) = \begin{cases} f(x) - d\Phi(x-1), & k=0, \\ 0, & k=1, \\ -S_{k-2,left}^{(4)}, & k \geq 2, \end{cases} \quad x \in (0,1), \quad (3a)$$

$$-bS_{k,right}''(x) + cS_{k,right}(x) = -dS_{k,left}(x-1) + \begin{cases} f(x), & k=0, \\ 0, & k=1, \\ -S_{k-2,right}^{(4)}, & k \geq 2, \end{cases} \quad x \in (1,2), \quad (3b)$$

$$S_{k,left}(0) = \begin{cases} 0, & k=0, \\ -E_{k,left}(0), & k \geq 1, \end{cases} \quad S_{k,right}(2) = \begin{cases} 0, & k=0, \\ -E_{k,right}(2), & k \geq 1, \end{cases} \quad (3c)$$

$$\llbracket S_k \rrbracket(1) = \begin{cases} 0, & k \leq 2, \\ -\llbracket W_k \rrbracket(1), & k \geq 3, \end{cases} \quad \llbracket S_k' \rrbracket(1) = \begin{cases} 0, & k \leq 1, \\ -\llbracket W_{k+1}' \rrbracket(1), & k \geq 2. \end{cases} \quad (3d)$$

The inner expansion for the left boundary layer solves for $\xi \in [0, \infty)$ and $k \geq 1$

$$\tilde{E}_{k,left}^{(4)}(\xi) - b\tilde{E}_{k,left}''(\xi) = \begin{cases} 0, & k \leq 2, \\ -c\tilde{E}_{k-2,left}(\xi), & k \geq 3, \end{cases} \quad (4a)$$

$$\tilde{E}_{k,left}'(0) = -S_k'(0), \text{ exp. decay}, \quad (4b)$$

while for the right boundary layer we have for $\eta \in [0, \infty)$ and $k \geq 1$

$$\tilde{E}_{k,right}^{(4)}(\eta) - b\tilde{E}_{k,right}''(\eta) = \begin{cases} 0, & k \leq 2, \\ -c\tilde{E}_{k-2,right}(\eta), & k \in \{3, 4\}, \\ -c\tilde{E}_{k-2,right}(\eta) - d\tilde{W}_{k-2,left}(\eta), & k \geq 5, \end{cases} \quad (5a)$$

$$\tilde{E}'_{k,right}(0) = -S'_k(2), \text{ exp. decay.} \quad (5b)$$

Finally, the inner expansion of the inner layer solves for $\psi, \theta \in [0, \infty)$ and $k \geq 3$

$$\tilde{W}_{k,left}^{(4)}(\psi) - b\tilde{W}_{k,left}''(\psi) = -d\tilde{E}_{k-2,right}(\psi) + \begin{cases} 0, & k \leq 4, \\ -c\tilde{W}_{k-2,left}(\psi), & k \geq 5, \end{cases} \quad (6a)$$

$$\tilde{W}_{k,right}^{(4)}(\theta) - b\tilde{W}_{k,right}''(\theta) = -d\tilde{E}_{k-2,left}(\theta) + \begin{cases} 0, & k \leq 4, \\ -c\tilde{W}_{k-2,right}(\theta), & k \geq 5, \end{cases} \quad (6b)$$

$$\tilde{W}_{k,left}''(0) = \tilde{W}_{k,right}''(0), \quad (6c)$$

$$-\tilde{W}_{k,left}'''(0) = \tilde{W}_{k,right}'''(0) - \llbracket S'''_{k-3} \rrbracket(1), \text{ exp. decay.} \quad (6d)$$

With these problems we can define V_k uniquely for any $k \geq 0$ and by above considerations, we have the formal solution decomposition

$$\begin{aligned} u(x) &= \sum_{k=0}^{\infty} V_k + \mathcal{O}\left(e^{-\frac{\beta}{\varepsilon}}\right) \\ &= \sum_{k=0}^{\infty} \varepsilon^k S_k(x) + \sum_{k=1}^{\infty} \varepsilon^k (E_{k,left}(x) + E_{k,right}(x)) + \sum_{k=3}^{\infty} \varepsilon^k W_k(x) + \mathcal{O}\left(e^{-\frac{\beta}{\varepsilon}}\right). \end{aligned}$$

In the case $m = 2$ the inner expansions of E_{left} and E_{right} start with $k = 2$, but otherwise the same derivation holds.

Lemma 2.1. *Let us consider the system (2a) and (2b) together with the more general conditions*

$$u_1(0) = \alpha_1, u_1(1) = \alpha_2, u_2(1) = \alpha_2 + \delta_1, u_2(2) = \alpha_3, \quad (7a)$$

$$u'_1(0) = \beta_1, u'_1(1) = \beta_2, u'_2(1) = \beta_2 + \delta_2, u'_2(2) = \beta_3, \quad (7b)$$

where $\alpha_1, \alpha_3, \beta_1, \beta_3, \delta_1, \delta_2$ are given parameters and α_2, β_2 are chosen, such that

$$\llbracket u'' \rrbracket(1) = \llbracket u''' \rrbracket(1) = 0. \quad (8)$$

Then it follows that

$$\|u\|_{L^\infty(0,2)} \lesssim \|f\|_{L^\infty(0,2)} + |\alpha_1| + |\alpha_3| + |\delta_1| + |\delta_2| + |\beta_1| + |\beta_3|.$$

Proof. The proof is rather technical and is deferred to the appendix. \square

Theorem 2.2. *The solution u of problem (1) can be written for $x \in \Omega$ as*

$$u(x) = S(x) + E_1(x) + E_2(x) + W_1(x) + W_2(x),$$

where we have for $0 \leq k \leq q + 1$

$$\begin{aligned} \|S^{(k)}\|_{L^2(0,1)} + \|S^{(k)}\|_{L^2(1,2)} &\lesssim 1, \\ |E_1^{(k)}(x)| &\lesssim \varepsilon^{m-k} e^{-\frac{\beta x}{\varepsilon}}, & |E_2^{(k)}(x)| &\lesssim \varepsilon^{m-k} e^{-\frac{\beta(2-x)}{\varepsilon}}, \\ |W_1^{(k)}(x)\chi_{(0,1)}(x)| &\lesssim \varepsilon^{3-k} e^{-\frac{\beta(1-x)}{\varepsilon}}, & |W_2^{(k)}(x)\chi_{(1,2)}(x)| &\lesssim \varepsilon^{3-k} e^{-\frac{\beta(x-1)}{\varepsilon}}. \end{aligned}$$

Proof. Using the decomposition

$$u(x) = \sum_{k=0}^{\ell} V_k(x) + R(x)$$

with the remainder R , we can consider the problem for $u - R$. Here we have

$$\begin{aligned} |(u - R)(0)| + |(u - R)(2)| &\lesssim \varepsilon^{\ell+1} \\ |(u - R)'(0)| + |(u - R)'(2)| &\lesssim e^{-\sqrt{b}/\varepsilon} \\ |[u - R]''(1)| &\lesssim \varepsilon^{\ell+3} \\ |[u - R]'''(1)| &\lesssim \varepsilon^{\ell+2} \\ \|L(u - R)\|_{L^\infty(0,2)} &\lesssim \varepsilon^{\ell+1}. \end{aligned}$$

Lemma 2.1 gives $\|u - R\|_{L^\infty(0,2)} \lesssim \varepsilon^{\ell+1}$ and the remainder can be incorporated into S together with the contributions S_0 to S_ℓ . Similarly we combine the different layer components into E_1 , E_2 , W_1 and W_2 and the proof is done by choosing ℓ large enough. \square

We will also denote the boundary layers by $E = E_1 + E_2$ and the inner layer by $W = W_1\chi_{(0,1)} + W_2\chi_{(1,2)}$. A visual confirmation is given for two examples in Figures 1 and 2 in Section 6.

3 Numerical method

To derive our numerical method, we introduce the auxiliary variable

$$w = \varepsilon u''.$$

Note that by Theorem 2.2 we immediately have a decomposition for w :

$$w = \tilde{S} + \tilde{E}_1 + \tilde{E}_2 + \tilde{W}_1 + \tilde{W}_2,$$

where for $0 \leq k \leq q + 1$ we have

$$\begin{aligned} |\tilde{S}^{(k)}(x)| &\lesssim \varepsilon, \\ |\tilde{E}_1^{(k)}(x)| &\lesssim \varepsilon^{m-1-k} e^{-\frac{\beta x}{\varepsilon}}, & |\tilde{E}_2^{(k)}(x)| &\lesssim \varepsilon^{m-1-k} e^{-\frac{\beta(2-x)}{\varepsilon}}, \\ |\tilde{W}_1^{(k)}(x)\chi_{(0,1)}(x)| &\lesssim \varepsilon^{2-k} e^{-\frac{\beta(1-x)}{\varepsilon}}, & |\tilde{W}_2^{(k)}(x)\chi_{(1,2)}(x)| &\lesssim \varepsilon^{2-k} e^{-\frac{\beta(x-1)}{\varepsilon}}. \end{aligned}$$

Similar to the previous notation we set $\tilde{E} = \tilde{E}_1 + \tilde{E}_2$ and $\tilde{W} = \tilde{W}_1\chi_{(0,1)} + \tilde{W}_2\chi_{(1,2)}$. Now we rewrite our problem (1) into its variational formulation. Let

$$\mathcal{U} := \begin{cases} H_0^1(\Omega) \times H^1(\Omega), & m = 1, \\ H_0^1(\Omega) \times H_0^1(\Omega), & m = 2. \end{cases}$$

Then the problem reads: Find $(u, w) \in \mathcal{U}$ such that for all $(y, z) \in \mathcal{U}$ it holds

$$\begin{aligned} B((u, w), (y, z)) &:= -\varepsilon \langle w', y' \rangle + \langle bu', y' \rangle + \langle b'u', y \rangle + \langle cu, y \rangle + \langle du(\cdot - 1), y \rangle_{(1,2)} \\ &\quad + \varepsilon \langle u', z' \rangle + \langle w, z \rangle \\ &= \langle f, y \rangle - \langle d\Phi(\cdot - 1), y \rangle_{(0,1)} =: F(y). \end{aligned} \quad (9)$$

Note that for $m = 1$ the normal-boundary condition is only weakly enforced. For the bilinear form defined in (9) we have coercivity

$$\begin{aligned} B((u, w), (u, w)) &:= -\varepsilon \langle w', u' \rangle + \langle bu', u' \rangle + \langle b'u', u \rangle + \langle cu, u \rangle + \langle du(\cdot - 1), u \rangle_{(1,2)} \\ &\quad + \varepsilon \langle u', w' \rangle + \langle w, w \rangle \\ &= \langle bu', u' \rangle + \langle b'u', u \rangle + \langle cu, u \rangle + \langle du(\cdot - 1), u \rangle_{(1,2)} + \langle w, w \rangle \\ &\geq \|w\|_{L^2}^2 + \frac{\beta^2}{2} \|u'\|_{L^2}^2 + \left(c - \frac{\|d\|_{L^\infty(1,2)}}{2} - \frac{\|b'\|_{L^\infty}^2}{2\beta^2} \right) \|u\|_{L^2}^2 \\ &\geq \|w\|_{L^2}^2 + \frac{\beta^2}{2} \|u'\|_{L^2}^2 + \delta \|u\|_{L^2}^2 =: |||(u, w)|||^2. \end{aligned} \quad (10)$$

Remark 3.1. Note that this norm is weak, i.e. contributions of the layers vanish for $\varepsilon \rightarrow 0$:

$$|||(S, \tilde{S})||| \lesssim 1, \quad |||(E, \tilde{E})||| \lesssim \varepsilon^{m-1/2} \rightarrow 0, \quad |||(W, \tilde{W})||| \lesssim \varepsilon^{5/2} \rightarrow 0.$$

Using weighted norms as in [9] only reduces the powers of ε , but the norm remains weak.

Our numerical method will be given on a layer-adapted mesh. We will start with an S-type mesh, see [13], in Section 4 and consider variations of it in Section 5. Let the number of mesh cells $N \in \mathbb{N}$ be divisible by 8 and

$$\lambda := \min \left\{ \frac{\sigma}{\beta} \varepsilon \ln(N), \frac{1}{4} \right\}$$

be the transition point, where we assume that ε is small enough such that $\lambda < \frac{1}{4}$. The parameter $\sigma > 0$ is defined in the following numerical analysis. The nodes of the mesh Ω_h are then given by

$$x_i = \begin{cases} \frac{\sigma\varepsilon}{\beta} \phi\left(\frac{4i}{N}\right), & 0 \leq i \leq \frac{N}{8}, \\ \frac{4i}{N}(1-2\lambda) + 2\lambda - \frac{1}{2}, & \frac{N}{8} \leq i \leq \frac{3N}{8}, \\ 1 - \frac{\sigma\varepsilon}{\beta} \phi\left(2 - \frac{4i}{N}\right), & \frac{3N}{8} \leq i \leq \frac{N}{2}, \\ 1 + x_{i-N/2}, & \frac{N}{2} \leq i \leq N. \end{cases} \quad (11)$$

We denote the so-called mesh-defining function by ϕ , which is monotonically increasing with $\phi(0) = 0$ and $\phi(1/2) = \ln(N)$, see [13] for the exact conditions on ϕ . In the numerical analysis we will also use the associated mesh characterising function $\psi = e^\phi$, or more precisely the quantity $\max |\psi'| := \max_{t \in [0, 1/2]} |\psi'(t)|$. Two of the most common S-type meshes are the Shishkin mesh with

$$\phi(t) = 2t \ln N, \quad \psi(t) = N^{-2t}, \quad \max |\psi'| \leq 2 \ln N, \quad h = \frac{8\sigma\varepsilon}{\beta} N^{-1} \ln N$$

and the Bakhvalov S-mesh with

$$\phi(t) = -\ln(1 - 2t(1 - N^{-1})), \quad \psi(t) = 1 - 2t(1 - N^{-1}), \quad \max |\psi'| \leq 2, \quad h \leq \frac{\sigma\varepsilon}{\beta} \ln 5.$$

For the mesh widths within the layers it holds, see [13],

$$h_i \lesssim \varepsilon N^{-1} \max |\psi'| e^{\frac{\beta x}{\sigma\varepsilon}}, \quad x \in [x_{i-1}, x_i].$$

The mesh Ω_h is then given by

$$\Omega_h := \{[x_{i-1}, x_i], i \in \{1, \dots, N\}\}.$$

Note that the maximum mesh width in the layer regions is $h \lesssim \varepsilon$ and outside $H \lesssim N^{-1}$. Finally, we define our discrete space on the given mesh by

$$\mathcal{U}_h := \{(u_h, w_h) \in \mathcal{U} : u_h|_T \in \mathbb{P}_q(T), w_h|_T \in \mathbb{P}_q(T), \forall T \in \Omega_h\},$$

where $\mathbb{P}_q(T)$ denotes the space of polynomials of maximum degree q over T . Our discrete method is given by: Find $(u_h, w_h) \in \mathcal{U}_h$ such that for all $(y, z) \in \mathcal{U}_h$ it holds

$$B((u_h, w_h), (y, z)) = F(y). \tag{12}$$

4 Numerical analysis

Note that by $\mathcal{U}_h \subset \mathcal{U}$, (9) and (12) we have Galerkin orthogonality

$$B((u - u_h, w - w_h), (y, z)) = 0, \quad \text{for all } (y, z) \in \mathcal{U}_h. \tag{13}$$

To analyse the error of the numerical method, we define a compound interpolation operator $I = (I_1, I_2) : C(\Omega)^2 \rightarrow \mathcal{U}_h$ locally for each $i \in \{1, \dots, N\}$ and $v \in C([x_{i-1}, x_i])$ by

$$(I_j v - v)(x_{i-1}) = 0, \quad (I_j v - v)(x_i) = 0, \\ \int_{x_{i-1}}^{x_i} (I_j v - v)(x) \xi(x) dx = 0, \quad \forall \xi \in \mathbb{P}_{q-2}([x_{i-1}, x_i]), \quad j \in \{1, 2\}.$$

Here I_1 and I_2 are defined similarly and for $m = 2$ they are the same, but for $m = 1$ the spaces the operator maps into are different. Let us decompose the errors as follows

$$\begin{aligned} u - u_h &= (u - I_1 u) - (u_h - I_1 u) =: \eta_u + \xi_u, \\ w - w_h &= (w - I_2 w) - (w_h - I_2 w) =: \eta_w + \xi_w, \end{aligned}$$

where (η_u, η_w) is the interpolation error and $(\xi_u, \xi_w) \in \mathcal{U}_h$ is the discrete error. Then with (13) and the coercivity (10) we obtain the error inequality

$$\|(\xi_u, \xi_w)\|^2 \leq B((\xi_u, \xi_w), (\xi_u, \xi_w)) = B((\eta_u, \eta_w), (\xi_u, \xi_w)).$$

Lemma 4.1. *It holds*

$$B((\eta_u, \eta_w), (\xi_u, \xi_w)) \lesssim (\|\eta_u\|_{L^2} + \|\eta_w\|_{L^2} + \|b - \bar{b}\|_{L^\infty} \|\eta'_u\|_{L^2}) \|(\xi_u, \xi_w)\|,$$

where \bar{b} is a cell-wise average of b .

Proof. Let us look at the individual terms of

$$\begin{aligned} B((\eta_u, \eta_w), (\xi_u, \xi_w)) &= -\varepsilon \langle \eta'_w, \xi'_u \rangle + \varepsilon \langle \eta'_u, \xi'_w \rangle + \langle b \eta'_u, \xi'_u \rangle + \langle b' \eta'_u, \xi_u \rangle + \langle c \eta_u, \xi_u \rangle + \langle \eta_w, \xi_w \rangle \\ &\quad + \langle d \eta_u(\cdot - 1), \xi_u \rangle_{(1,2)} \\ &=: \sum_{k=1}^7 B_k \end{aligned}$$

on each cell $T_i := [x_{i-1}, x_i]$. By definition of the interpolation operator I and integration by parts we obtain

$$\begin{aligned} \langle \eta'_w, \xi'_u \rangle_{T_i} &= \eta_w(x) \xi'_u(x) \Big|_{x_{i-1}}^{x_i} - \int_{x_{i-1}}^{x_i} \eta_w(x) \xi''_u(x) dx = 0, \\ \langle \eta'_u, \xi'_w \rangle_{T_i} &= 0 \end{aligned}$$

and therefore, B_1 and B_2 are zero. For B_3 we introduce the cell-wise average

$$\bar{b}|_{T_i} = \int_{T_i} b(x) dx.$$

Then it holds again with the interpolation property

$$\langle b \eta'_u, \xi'_u \rangle = \langle (b - \bar{b}) \eta'_u, \xi'_u \rangle + \bar{b} \langle \eta'_u, \xi'_u \rangle \lesssim \|b - \bar{b}\|_{L^\infty(T_i)} \|\eta'_u\|_{L^2(T_i)} \|\xi'_u\|_{L^2(T_i)}.$$

For B_4 we also apply integration by parts and have

$$\begin{aligned} \langle b' \eta'_u, \xi_u \rangle_{T_i} &= \eta_u(x) b'(x) \xi_u(x) \Big|_{x_{i-1}}^{x_i} - \langle b'' \eta_u, \xi_u \rangle_{T_i} - \langle b' \eta_u, \xi'_u \rangle_{T_i} \\ &\lesssim \|\eta_u\|_{L^2(T_i)} (\|\xi_u\|_{L^2(T_i)} + \|\xi'_u\|_{L^2(T_i)}). \end{aligned}$$

The last three terms B_5 to B_7 are simply estimated by a Cauchy-Schwarz inequality

$$\begin{aligned} \langle c \eta_u, \xi_u \rangle &\lesssim \|\eta_u\|_{L^2} \|\xi_u\|_{L^2}, \\ \langle \eta_w, \xi_w \rangle &\lesssim \|\eta_w\|_{L^2} \|\xi_w\|_{L^2}, \\ \langle d \eta_u(\cdot - 1), \xi_u \rangle_{(1,2)} &\lesssim \|\eta_u\|_{L^2(0,1)} \|\xi_u\|_{L^2(1,2)}. \end{aligned}$$

Combining the local and global estimates completes the proof. \square

The main ingredient of interpolation error estimates are local estimates. Here we have on a cell τ_i of width h_i

$$\|(v - Iv)^{(\ell)}\|_{L^2(\tau_i)} \lesssim \|h_i^{s-\ell} v^{(s)}\|_{L^2(\tau_i)} \quad (14)$$

for $0 \leq \ell < s \leq q + 1$.

Lemma 4.2. *It holds for $u, w \in H^{q+1}(\Omega)$ and $\sigma \geq q + 1$ using the results of Section 2*

$$\begin{aligned} \|\eta_u\|_{L^2} &\lesssim (h + N^{-1})^{q+1} + \varepsilon^m (N^{-1} \max |\psi'|)^{q+1}, \\ \|\eta_w\|_{L^2} &\lesssim \varepsilon (h + N^{-1})^{q+1} + \varepsilon^{m-1} (N^{-1} \max |\psi'|)^{q+1}, \\ \|\eta'_u\|_{L^2} &\lesssim (h + N^{-1})^q + \varepsilon^{m-1/2} (N^{-1} \max |\psi'|)^q. \end{aligned}$$

Proof. Interpolation error estimation of I on an S-type mesh is standard, see [13]. Nevertheless, we present it here again to highlight the changes we make in Section 5 on coarsened S-type meshes.

With (14) for S and \tilde{S} we obtain the estimates

$$\begin{aligned} \|S - I_1 S\|_{L^2} &\lesssim (h + N^{-1})^{q+1}, & \|\tilde{S} - I_2 \tilde{S}\|_{L^2} &\lesssim \varepsilon (h + N^{-1})^{q+1}, \\ \|(S - I_1 S)'\|_{L^2} &\lesssim (h + N^{-1})^q. \end{aligned}$$

For the boundary layer E_1 (and similarly for E_2) we use additionally the L^∞ -stability of I and the choice of the transition point λ of the mesh. We get

$$\begin{aligned} \|E_1 - I_1 E_1\|_{L^2}^2 &= \|E_1 - I_1 E_1\|_{L^2(0,\lambda)}^2 + \|E_1 - I_1 E_1\|_{L^2(\lambda,2)}^2 \\ &\lesssim \sum_{\tau_i \in \Omega_h([0,\lambda])} (\varepsilon N^{-1} \max |\psi'|)^{2(q+1)} \varepsilon^{2(m-(q+1))} \|e^{(\frac{q+1}{\sigma}-1)\frac{x\beta}{\varepsilon}}\|_{L^2(\tau_i)}^2 + \|E_1\|_{L^\infty(\lambda,2)}^2 \\ &\lesssim \varepsilon^{2m} ((N^{-1} \max |\psi'|)^{q+1} + N^{-2\sigma}) \lesssim \varepsilon^{2m} (N^{-1} \max |\psi'|)^{q+1} \end{aligned}$$

due to $\sigma \geq q + 1$. Note, that for $\sigma > q + 1$ we could gain another half power of ε . For E_2 we get the same result and for W we have to replace m with 2. Similarly we have

$$\|\tilde{E} - I_2 \tilde{E}\|_{L^2} \lesssim \varepsilon^{m-1} (N^{-1} \max |\psi'|)^{q+1}, \quad \|\tilde{W} - I_2 \tilde{W}\|_{L^2((0,1) \cup (1,2))} \lesssim \varepsilon^2 (N^{-1} \max |\psi'|)^{q+1}.$$

These estimates give the first two results of the lemma. To estimate the derivative of the interpolation error, we demonstrate the procedure only for E_1 , the others follow similarly. It holds

$$\begin{aligned} \|(E_1 - I_1 E_1)'\|_{L^2(0,\lambda)}^2 &\lesssim \sum_{\tau_i \in \Omega_h([0,\lambda])} (\varepsilon N^{-1} \max |\psi'|)^{2q} \varepsilon^{2(m-(q+1))} \|e^{(\frac{q}{\sigma}-1)\frac{x\beta}{\varepsilon}}\|_{L^2(\tau_i)}^2 \\ &\lesssim \varepsilon^{2m-1} (N^{-1} \max |\psi'|)^{2q}, \\ \|(E_1 - I_1 E_1)'\|_{L^2(\lambda,1-\lambda)} &\lesssim \|E_1'\|_{L^2(\lambda,1-\lambda)} + N \|I_1 E_1\|_{L^2(\lambda,1-\lambda)} \\ &\lesssim \varepsilon^{m-1/2} N^{-\sigma} + N^{1-\sigma} \varepsilon^m. \end{aligned}$$

In the remaining parts of Ω we use one of the two techniques above, depending on the local mesh. The other layer parts can be estimated similarly and the proof is complete. \square

Combining the previous lemmas yields the convergence result in the energy norm.

Theorem 4.3 (Supercloseness and convergence). *For the solutions $(u, w) \in \mathcal{U}$ of (9) and $(u_h, w_h) \in \mathcal{U}_h$ of (12) it holds under the assumptions $u, w \in H^{q+1}(\Omega)$ and $\sigma \geq q + 1$, the supercloseness result*

$$\| (I_1 u - u_h, I_2 w - w_h) \| \lesssim (h + N^{-1} \max |\psi'|)^{q+1}$$

and the convergence result

$$\| (u - u_h, w - w_h) \| \lesssim (h + N^{-1} \max |\psi'|)^q.$$

Proof. Substituting the interpolation error estimates into Lemma 4.1 gives the supercloseness result. This, together with a triangle inequality and the interpolation error again, gives the convergence result. \square

Remark 4.4. *Since the discrete error converges with a higher order than the error itself, we have a supercloseness phenomenon. We can exploit this by applying a post-processing with an interpolation on a macro mesh of the discrete solution into a polynomial space of one degree higher, see e.g. [5, 15] for a 2d setting of this approach. The post-processed solution then converges with order $q+1$ (assuming $\sigma \geq q+2$ and regularity of the solution). We also obtain optimal error convergence in the L^2 -norm*

$$\begin{aligned} \|u - u_h\|_{L^2} + \|w - w_h\|_{L^2} &\leq \|\eta_u\|_{L^2} + \|\xi_u\|_{L^2} + \|\eta_w\|_{L^2} + \|\xi_w\|_{L^2} \\ &\lesssim (h + N^{-1} \max |\psi'|)^{q+1}. \end{aligned}$$

5 Coarser meshes

According to our solution decomposition the inner layers W and \tilde{W} are weak layers and we will modify the meshes near $x = 1$. Note that E and \tilde{E} are also weak layers and similar approaches can be used for them near the boundary.

5.1 Weak equidistant mesh

In [3] the solution also contained a weak layer. This allowed a modification of the mesh in order to coarsen the layer part of the mesh. We will apply this mesh idea here too, adapted to the even weaker inner layer. As mentioned above, this could also be done for the boundary layers.

Let us define a second transition point in addition to the transition point λ

$$\mu := \begin{cases} \frac{1}{4}, & q \leq 2, \\ \min \left\{ \frac{\varepsilon^{1-\frac{5}{2(q+1)}}}{\beta}, \frac{1}{4} \right\}, & q > 2. \end{cases}$$

For $q > 2$ we assume ε to be small enough such that $\mu < \frac{1}{4}$. We then use an S-type mesh with $N/8$ cells in each $(0, \lambda)$ and $(2 - \lambda, 2)$ as before, and choose equidistant meshes in

$(\lambda, 1 - \mu)$, $(1 - \mu, 1 + \mu)$ and $(1 + \mu, 2 - \lambda)$ with $N/4$ cells each. Let \tilde{h} denote the mesh width in $(1 - \mu, 1 + \mu)$. For it holds

$$\tilde{h} \lesssim \begin{cases} N^{-1}, & q \leq 2, \\ N^{-1} \varepsilon^{1 - \frac{5}{2(q+1)}}, & q > 2 \end{cases} \Rightarrow \tilde{h} \lesssim N^{-1}.$$

According to the previous analysis, we only need to estimate the interpolation error on this mesh in order to obtain the approximation error and the convergence error.

Lemma 5.1. *Assuming $e^{-\varepsilon^{-1/q}} \leq (h + N^{-1})^{q-2}$, we have on a mesh consisting of an S -type mesh with $\sigma \geq q + 1$ for the boundary layers and an equidistant weak mesh for the interpolation operator I*

$$\begin{aligned} \|u - I_1 u\|_{L^2} &\lesssim (h + N^{-1})^{q+1} + \varepsilon (N^{-1} \max |\psi'|)^{q+1}, \\ \|w - I_2 w\|_{L^2} &\lesssim (h + N^{-1})^{q+1/2}, \\ \|(u - I_1 u)'\|_{L^2} &\lesssim (h + N^{-1})^q + \varepsilon^{1/2} (N^{-1} \max |\psi'|)^q. \end{aligned}$$

Proof. The estimates for S , \tilde{S} , E and \tilde{E} are as in Lemma 4.2, also for the derivatives. So we only need to look at the inner layers. For \tilde{W} we distinguish between the polynomial degrees. For $q = 1$ we estimate directly with (14) and $s = 2$

$$\|\tilde{W} - I_2 \tilde{W}\|_{L^2} \lesssim (h + N^{-1})^2 \|(\tilde{W})''\|_{L^2} \lesssim \varepsilon^{1/2} (h + N^{-1})^2$$

and for $q = 2$ we use $s = 2$ and $s = 3$ together

$$\|\tilde{W} - I_2 \tilde{W}\|_{L^2} \lesssim ((h + N^{-1})^2 \|(\tilde{W})''\|_{L^2})^{1/2} ((h + N^{-1})^3 \|(\tilde{W})'''\|_{L^2})^{1/2} \lesssim (h + N^{-1})^{5/2}.$$

For $q > 2$ the same trick can be applied outside the inner layer region,

$$\begin{aligned} \|\tilde{W} - I_2 \tilde{W}\|_{L^2((0,1-\mu) \cap (1+\mu,2))} &\lesssim (N^{-2} \|(\tilde{W})''\|_{L^2((0,1-\mu) \cap (1+\mu,2))})^{1/2} \\ &\quad (N^{-3} \|(\tilde{W})'''\|_{L^2((0,1-\mu) \cap (1+\mu,2))})^{1/2} \\ &\lesssim N^{-5/2} e^{-\varepsilon^{-1/q}} \lesssim N^{-(q+1/2)}, \end{aligned}$$

while inside we estimate

$$\|\tilde{W} - I_2 \tilde{W}\|_{L^2(1-\mu,1+\mu)} \lesssim \tilde{h}^{q+1} \|\tilde{W}^{(q+1)}\|_{L^2(1-\mu,1+\mu)} \lesssim N^{-(q+1)} \varepsilon^{q+1 - \frac{5}{2}} \varepsilon^{3/2 - q} \lesssim N^{-(q+1)}.$$

For W it follows by the same steps

$$\|W - I_1 W\|_{L^2} \lesssim (h + N^{-1})^{q+1},$$

using (14) with $s = 3$ and $s = 4$ where appropriate. The estimation of the derivative follows also the same steps and we obtain

$$\|(W - I_1 W)'\|_{L^2} \lesssim (h + N^{-1})^q.$$

Combining all these estimates completes the proof. \square

The convergence proof is now a straightforward consequence.

Theorem 5.2. *Under the conditions $\sigma \geq q+1$ and $e^{-\varepsilon^{-1/q}} \leq (h + N^{-1})^{q-2}$ it holds for the exact solution (u, w) of (9) and the discrete solution (u_h, w_h) of (12) the supercloseness estimate*

$$\| (I_1 u - u_h, I_2 w - w_h) \| \lesssim (h + N^{-1} \max |\psi'|)^{q+1/2}$$

and the convergence estimate

$$\| (u - u_h, w - w_h) \| \lesssim (h + N^{-1} \max |\psi'|)^q.$$

Remark 5.3. *The condition $e^{-\varepsilon^{-1/q}} \leq (h + N^{-1})^{q-2}$ limits the applicability of the mesh for higher values of q and small ε , see also [3], where the condition was similar. For $q \leq 2$ we have no restriction, and for $q = 3$ the condition is satisfied for reasonable choices of N and ε . Nevertheless, for $q > 2$ in the next subsection we provide another coarse mesh which does not restrict the choices of N and ε .*

5.2 Weak S-type mesh

In this section we use an S-type mesh for the inner layer in the case of $q > 2$, but we modify its transition point with respect to the weak layer. Let

$$\nu := \min \left\{ \frac{\sigma}{\beta} \varepsilon^{1 - \frac{5}{2(q+1)}} \ln N, \frac{1}{4} \right\} \geq \lambda$$

and the mesh is defined as in (11) with the obvious modification of using ν instead of λ near $x = 1$. One consequence is the following bound on the mesh width h_i in the inner layer region

$$h_i \leq \frac{\sigma}{\beta} \varepsilon^{\frac{2q-3}{2(q+1)}} N^{-1} \max |\psi'| \exp \left(\frac{\beta x}{\sigma} \varepsilon^{-\frac{2q-3}{2(q+1)}} \right) \lesssim \tilde{h}$$

for $x \in (x_{i-1}, x_i)$ and the maximum mesh width $h \lesssim \tilde{h} \lesssim \varepsilon^{1 - \frac{5}{2(q+1)}}$.

As in the previous section, we will first look at the interpolation error.

Lemma 5.4. *Let $\sigma \geq q+1$. Then we have for the interpolation operator I on the weak S-type mesh*

$$\begin{aligned} \|u - I_1 u\|_{L^2} &\lesssim (\tilde{h} + N^{-1} \max |\psi'|)^{q+1}, \\ \|w - I_2 w\|_{L^2} &\lesssim (\tilde{h} + N^{-1} \max |\psi'|)^{q+1}, \\ \|(u - I_1 u)'\|_{L^2} &\lesssim (\tilde{h} + N^{-1} \max |\psi'|)^q. \end{aligned}$$

Proof. As for Lemma 5.1, we only need to estimate the interpolation errors for the inner layers. The estimates for the remaining terms only need to be modified by using $h \lesssim \tilde{h}$ due to the new maximum mesh width in the inner layer region.

For \tilde{W} we obtain in the layer region with (14)

$$\begin{aligned} \|\tilde{W} - I_2\tilde{W}\|_{L^2(1-\nu,1)}^2 &\lesssim \sum_{\tau_i \in \Omega_h([1-\nu,1])} \|h_i^{q+1}\tilde{W}_1^{(q+1)}\|_{L^2(\tau_i)}^2 \\ &\lesssim \varepsilon^{-1}(N^{-1}\max|\psi'|)^{2(q+1)} \left\| \exp\left(\left(\frac{q+1}{\sigma\varepsilon^{\frac{2q-3}{2(q+1)}}} - \frac{1}{\varepsilon}\right)\beta x\right) \right\|_{L^2(1-\nu,1)}^2 \\ &\lesssim (N^{-1}\max|\psi'|)^{2(q+1)} \end{aligned}$$

due to $\sigma \geq q+1$ and $\varepsilon^{\frac{2q-3}{2(q+1)}} = \varepsilon^{1-\frac{5}{2(q+1)}} > \varepsilon$. In the other layer region the same result holds. Outside the layer region we have by $\nu > \lambda$ and the L^∞ -stability of the interpolation operator

$$\|\tilde{W} - I_2\tilde{W}\|_{L^2((0,1-\nu)\cap(1+\nu,2))} \lesssim \|\tilde{W}\|_{L^\infty((0,1-\nu)\cap(1+\nu,2))} \lesssim |\tilde{W}(1-\nu)| \lesssim |\tilde{W}(1-\lambda)| \lesssim \varepsilon^2 N^{-\sigma}.$$

For W we obtain analogously

$$\|W - I_1W\|_{L^2} \lesssim \varepsilon^2 (N^{-1}\max|\psi'|)^{q+1}.$$

Thus, the first two estimates are proven. For the derivative we look at $(0, \lambda)$, $(\lambda, 1-\nu)$ and $(1-\nu, 1)$ separately:

$$\begin{aligned} \|(W_1 - I_1W_1)'\|_{L^2(0,\lambda)} &\lesssim h^q \|W_1^{(q+1)}\|_{L^2(0,\lambda)} \lesssim \varepsilon^q |W_1^{(q+1)}(1-\lambda)| \lesssim \varepsilon^2 N^{-\sigma}, \\ \|(W_1 - I_1W_1)'\|_{L^2(\lambda,1-\nu)} &\lesssim \|W_1'\|_{L^2(\lambda,1-\nu)} + N \|W_1\|_{L^\infty(\lambda,1-\nu)} \lesssim \varepsilon^{5/2} N^{-\sigma} + \varepsilon^3 N^{-(\sigma-1)}, \\ \|(W_1 - I_1W_1)'\|_{L^2(1-\nu,1)} &\lesssim \varepsilon^{\frac{2q-3}{2(q+1)}q} (N^{-1}\max|\psi'|)^q \varepsilon^{1-q} \left\| \exp\left(\left(\frac{q}{\sigma\varepsilon^{\frac{2q-3}{2(q+1)}}} - \frac{1}{\varepsilon}\right)\right) \right\|_{L^2(1-\nu,1)} \\ &\lesssim \varepsilon^{\frac{5}{2(q+1)}} (N^{-1}\max|\psi'|)^q. \end{aligned}$$

On the other parts of the domain we get the same bounds. When estimating $(S - I_1S)'$ we can proceed as before, but for $(E - I_1E)'$ we have to be careful in the middle layer region. Direct estimation using (14) with $s = 2$ works for $q > 1$, but using the W_1^∞ -stability of I_1 works for all q :

$$\|(E_1 - I_1E_1)'\|_{L^2(1-\nu,1)} \lesssim \|E_1'\|_{L^2(1-\nu,1)} + \nu^{1/2} \|E_1'\|_{L^\infty(1-\nu,1)} \lesssim \varepsilon^{m-1} N^{-\sigma} \lesssim N^{-\sigma}$$

due to $m \geq 1$. Combining all estimates finishes the proof. \square

With the interpolation error result we obtain virtually the same result as in Theorem 4.3.

Theorem 5.5 (Supercloseness and convergence). *For the solutions $(u, w) \in \mathcal{U}$ of (9) and $(u_h, w_h) \in \mathcal{U}_h$ of (12) it holds under the assumptions $u, w \in H^{q+1}(\Omega)$ and $\sigma \geq q+1$, the supercloseness result*

$$\|(I_1u - u_h, I_2w - w_h)\| \lesssim (\tilde{h} + N^{-1}\max|\psi'|)^{q+1}$$

and the convergence result

$$\|(u - u_h, w - w_h)\| \lesssim (\tilde{h} + N^{-1}\max|\psi'|)^q.$$

Remark 5.6. *Let us compare the two coarser meshes for the inner layers and the results on them.*

- *The weak equidistant mesh is structurally simpler.*
- *In terms of size with respect to ε , the transition points μ and ν are of the same size.*
- *On both meshes convergence of order q is proved.*
- *On the weak S -type mesh we have supercloseness of order $q + 1$, while on the weak equidistant mesh we can only prove the order $q + 1/2$.*
- *The maximum mesh size \tilde{h} on weak S -type meshes is for optimal meshes, such as the Bakhvalov S -mesh, of order $\mathcal{O}\left(\varepsilon^{1-\frac{5}{2(q+1)}}\right)$. Then we have optimal convergence for $\varepsilon \lesssim N^{-(1+\frac{4}{2q-3})}$.*

As a result, a practical guide for the inner layer is to use

- *for arbitrary ε and $q \leq 2$ a piecewise equidistant mesh,*
- *for small ε and $q = 3$ a weak equidistant mesh and*
- *otherwise a weak S -type or a classical S -type mesh.*

Using a classical Shishkin mesh for the inner layer in the case of $q \geq 3$ will also yield optimal convergence results (without a logarithmic factor) under the assumption that

$$\varepsilon \lesssim (\ln N)^{-\frac{2q}{5}}$$

which is slightly stronger than

$$\lambda \leq \frac{1}{4} \quad \Rightarrow \quad \varepsilon \lesssim (\ln N)^{-1}$$

but much weaker than $\varepsilon \lesssim N^{-1}$.

6 Numerical experiments

We consider as first example in Ω

$$\varepsilon^2 u^{(4)}(x) - u''(x) + 2u(x) + u(x-1) = 5 \tag{15}$$

with $u(0) = u'(0) = u(2) = u'(2) = 0$, thus $m = 1$, and $\Phi(x) = 0$ for $x \in (-1, 0)$. Figure 1 shows the solution u and its first three derivatives. It is easy to see, that u' has two boundary layers and u''' an inner layer, visible in the zoom.

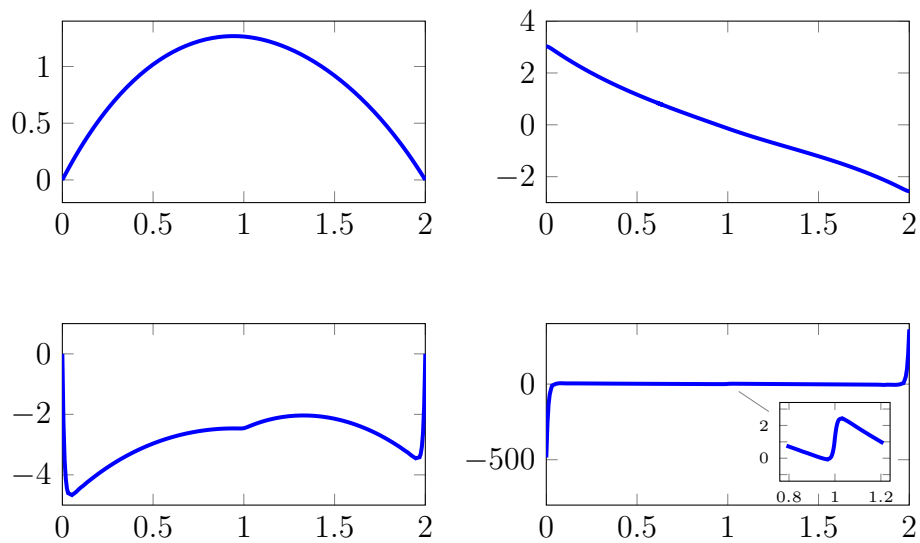


Figure 1: Solution u and u' , u'' , u''' (left to right, top to bottom), for example (15) with $\varepsilon = 10^{-2}$.

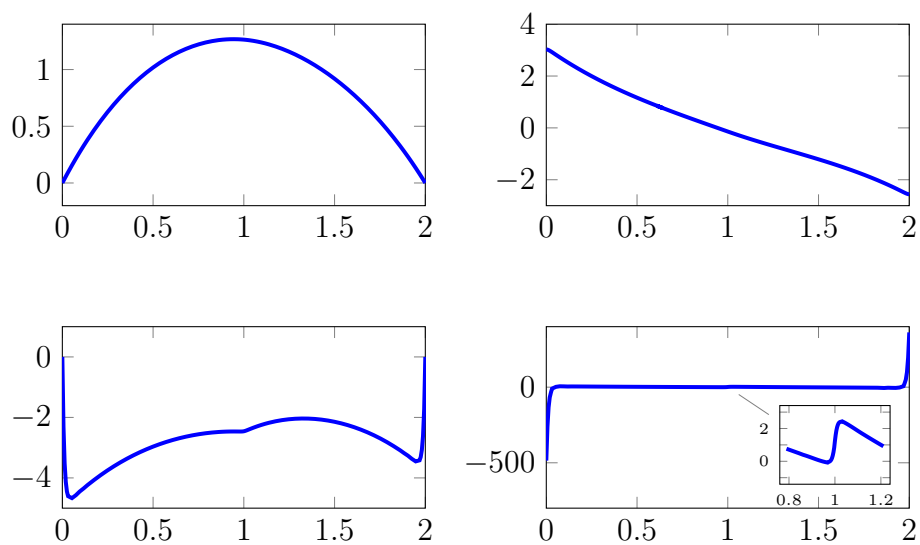


Figure 2: Solution u and u' , u'' , u''' (left to right, top to bottom), for example (16) with $\varepsilon = 10^{-2}$.

Our second example is almost the same, except for the boundary conditions. We consider in Ω

$$\varepsilon^2 u^{(4)}(x) - u''(x) + 2u(x) + u(x-1) = 5 \quad (16)$$

with $u(0) = u''(0) = u(2) = u''(2) = 0$, thus $m = 2$, and $\Phi(x) = 0$ for $x \in (-1, 0)$. Figure 2 shows the solution u and its first three derivatives. We see, that now u'' has two

Table 1: Errors for example (15) and $\varepsilon = 10^{-4}$ on a Bakhvalov S-type mesh for all layers.

q	N	$ (u - u_h, w - w_h) $		$\ u - u_h\ _{L^2}$		$\ w - w_h\ _{L^2}$	
1	64	5.27e-02	1.00	1.10e-03	2.00	3.19e-04	1.90
	128	2.64e-02	1.00	2.75e-04	2.00	8.54e-05	1.92
	256	1.32e-02		6.87e-05		2.26e-05	
2	64	4.51e-04	2.00	5.60e-06	3.00	4.18e-05	2.86
	128	1.12e-04	2.00	7.00e-07	3.00	5.77e-06	2.89
	256	2.81e-05		8.76e-08		7.78e-07	
3	64	1.66e-05	3.00	5.28e-08	2.93	3.18e-06	3.84
	128	2.08e-06	2.99	6.92e-09	0.23	2.22e-07	3.88
	256	2.61e-07		5.90e-09		1.50e-08	
4	16	3.41e-04	4.02	1.36e-07	4.18	1.76e-04	4.61
	32	2.10e-05	4.00	7.51e-09	0.26	7.22e-06	4.76
	64	1.32e-06	3.97	6.25e-09	0.09	2.66e-07	4.84
	128	8.40e-08	2.74	5.86e-09	-0.04	9.31e-09	4.77
	256	1.26e-08		6.01e-09		3.41e-10	

Table 2: Errors for example (15), $q = 2$ and $\varepsilon = 10^{-4}$ on different meshes.

N	BS-BS		BS-Shishkin		BS-weakeq		BS-weakShishkin	
64	4.51e-04	2.00	4.51e-04	2.00	4.43e-04	2.00	3.60e-04	2.06
128	1.12e-04	2.00	1.12e-04	2.00	1.11e-04	2.00	8.66e-05	2.05
256	2.81e-05		2.81e-05		2.77e-05		2.09e-05	

boundary layers and u''' still has an inner layer, visible in the zoom.

For our simulations we use the Matlab finite element suite `SOFE`¹ and all computations are done in double precision. Table 1 shows the results on a mesh consisting of Bakhvalov S-type meshes for all layers. We can confirm the predictions made in Theorem 4.3 of convergence in the $|||\cdot|||$ -norm of order q . Moreover, Remark 4.4 mentions as consequence of a supercloseness result an optimal error convergence in L^2 of order $q + 1$. This can also be observed in Table 1. Note that for higher values of N and higher polynomial degrees we have a collapse of the computational accuracy. This is a well-known phenomenon in singularly perturbed problems, and we cannot achieve machine precision. To get around this, we would have to use quadruple or arbitrary precision.

In Table 2 we compare the results on different meshes. We restrict the polynomial degree to $q = 2$ and look only at the $|||\cdot|||$ -norm. If we use a Bakhvalov S-mesh for the boundary layer it does not matter whether we use a Bakhvalov S-mesh or a Shishkin mesh for the inner layer. The results are the same. However, for $q = 2$ we can also use an equidistant

¹github.com/SOFE-Developers/SOFE

mesh for the inner layer and get slightly better results. Even better results can be obtained by using a weak S-type mesh, such as a weak Shishkin mesh. But overall they all perform similarly well and we observe convergence of order $q = 2$.

For example (16) we can do the same experiments and observe similar results. We only show the results corresponding to Table 2 in Table 3.

Table 3: Errors for example (16), $q = 2$ and $\varepsilon = 10^{-4}$ on different meshes.

N	BS-BS		BS-weakeq		BS-weakShishkin	
64	4.12e-04	2.00	4.04e-04	2.00	3.10e-04	2.07
128	1.03e-04	2.00	1.01e-04	2.00	7.38e-05	2.07
256	2.57e-05		2.52e-05		1.75e-05	

References

- [1] K. Bansal, P. Rai, and K.K. Sharma. Numerical treatment for the class of time dependent singularly perturbed parabolic problems with general shift arguments. *Differ. Equ. Dyn. Syst.*, 25(2):327–346, 2017.
- [2] M. Brdar, S. Franz, L. Ludwig, and H.-G. Roos. A balanced norm error estimation for the time-dependent reaction-diffusion problem with shift in space. *Appl. Math. Comp.*, (437):127507, 2023. <https://doi.org/10.1016/j.amc.2022.127507>.
- [3] M. Brdar, S. Franz, L. Ludwig, and H.-G. Roos. Numerical analysis of a singularly perturbed convection diffusion problem with shift in space. *Appl. Numer. Math.*, (186):129–142, 2023. <https://doi.org/10.1016/j.apnum.2023.01.003>.
- [4] P.P. Chakravarthy and K. Kumar. An adaptive mesh method for time dependent singularly perturbed differential-difference equations. *Nonlinear Engineering*, 8:328–339, 2019.
- [5] S. Franz. Superconvergence using pointwise interpolation in convection-diffusion problems. *Appl. Numer. Math.*, 76:132–144, 2014. corrected version: <https://arxiv.org/abs/1304.7443>.
- [6] V. Gupta, M. Kumar, and S. Kumar. Higher order numerical approximation for time dependent singularly perturbed differential-difference convection-diffusion equations. *Numer. Methods Partial Differential Equations*, 34:357–380, 2018.
- [7] D. Kumar and M.K. Kadalbajoo. A parameter-uniform numerical method for time-dependent singularly perturbed differential-difference equations. *Appl. Math. Model.*, 35:2805–2819, 2011.

- [8] D. Kumar and P. Kumari. Parameter-uniform numerical treatment of singularly perturbed initial-boundary value problems with large delay. *Appl. Numer. Math.*, 153:412–429, 2020.
- [9] N. Madden and M. Stynes. A weighted and balanced FEM for singularly perturbed reaction-diffusion problems. *Calcolo*, 58(2):Paper No. 28, 16, 2021.
- [10] M. A. Naimark. *Linear differential operators. Part I: Elementary theory of linear differential operators*. Frederick Ungar Publishing Co., New York, 1967.
- [11] S. Nicaise and Chr. Xenophontos. Robust approximation of singularly perturbed delay differential equations by the *hp* finite element method. *Comput. Methods Appl. Math.*, 13(1):21–37, 2013.
- [12] P. Rai and K. K. Sharma. Singularly perturbed convection-diffusion turning point problem with shifts. In *Mathematical analysis and its applications*, volume 143 of *Springer Proc. Math. Stat.*, pages 381–391. Springer, New Delhi, 2015.
- [13] H.-G. Roos and T. Linß. Sufficient conditions for uniform convergence on layer-adapted grids. *Computing*, 63:27–45, 1999.
- [14] H.-G. Roos, M. Stynes, and L. Tobiska. *Robust numerical methods for singularly perturbed differential equations*, volume 24 of *Springer Series in Computational Mathematics*. Springer-Verlag, Berlin, second edition, 2008.
- [15] M. Stynes and L. Tobiska. The SDFEM for a convection-diffusion problem with a boundary layer: optimal error analysis and enhancement of accuracy. *SIAM J. Numer. Anal.*, 41(5):1620–1642, 2003.
- [16] V. Subburayan and N. Ramanujam. Asymptotic initial value technique for singularly perturbed convection-diffusion delay problems with boundary and weak interior layers. *Appl. Math. Lett.*, 25(12):2272–2278, 2012.
- [17] V. Subburayan and N. Ramanujam. An initial value technique for singularly perturbed convection-diffusion problems with a negative shift. *J. Optim. Theory Appl.*, 158(1):234–250, 2013.

A Proof of Lemma 2.1

The proof of Lemma 2.1 relies on properties of an associated Green’s function that we will derive now.

Let G be the Green’s function defined for all $t \in (0, 1)$ by

$$\varepsilon^2 \partial_x^4 G(x, t) - b \partial_x^2 G(x, t) + c G(x, t) = \delta(x - t), \quad x \in \Omega = (0, 1), \quad (17a)$$

$$G(0, t) = G(2, t) = 0, \quad (17b)$$

$$G_x(0, t) = G_x(2, t) = 0. \quad (17c)$$

The characteristic solutions of (17a) are given by

$$y_1(x) = e^{-\mu_1 x}, y_2(x) = e^{-\mu_2 x}, y_3(x) = e^{-\mu_1(1-x)}, y_4(x) = e^{-\mu_2(1-x)},$$

where

$$\mu_1 = \sqrt{\frac{b + \sqrt{b^2 - 4\varepsilon^2 c}}{2\varepsilon^2}} \sim \sqrt{b}\varepsilon^{-1}, \mu_2 = \sqrt{\frac{b + \sqrt{b^2 - 4\varepsilon^2 c}}{2\varepsilon^2}} \sim \sqrt{\frac{c}{b}}.$$

We find a representation of G , see e.g. [10, Sec. 3.3], using

$$G(x, t) = \begin{cases} \sum_{i=1}^4 c_i^\ell(t) y_i(x), & x < t, \\ \sum_{i=1}^4 c_i^r(t) y_i(x), & x \geq t, \end{cases}$$

where the unknowns c_i^ℓ and c_i^r for each t can be found by solving the system

$$\begin{aligned} G(0, t) = 0, & \quad G(1, t) = 0, & \quad G_x(0, t) = 0, & \quad G_x(1, t) = 0, \\ \llbracket G \rrbracket(t, t) = 0, & \quad \llbracket G_x \rrbracket(t, t) = 0, & \quad \llbracket G_{xx} \rrbracket(t, t) = 0, & \quad \llbracket G_{xxx} \rrbracket(t, t) = \varepsilon^{-2}. \end{aligned}$$

These linearly independent conditions determine $G(x, t)$ uniquely for each $t \in (0, 1)$.

Now we want to represent u_1 and u_2 using G . For this purpose we define by $\Phi_i, i \in \{1, \dots, 4\}$ the Hermite basis of $\mathbb{P}_3(0, 1)$ associated with the evaluation of function and first derivative values and interpolate the boundary conditions in (7) by

$$\phi_1(x) = \alpha_1 \Phi_1(x) + \alpha_2 \Phi_2(x) + \beta_1 \Phi_3(x) + \beta_2 \Phi_4(x), \quad x \in (0, 1),$$

$$\phi_2(x) = (\alpha_2 + \delta_1) \Phi_1(x - 1) + \alpha_3 \Phi_2(x - 1) + (\beta_2 + \delta_2) \Phi_3(x - 1) + \beta_3 \Phi_4(x - 1), \quad x \in (1, 2).$$

Then $v_i := u_i - \phi_i$ satisfies homogeneous boundary conditions and we can reformulate the continuity conditions (8) for finding α_2 and β_2 as

$$\begin{aligned} \llbracket v'' \rrbracket(1) &= \phi_2''(1) - \phi_1''(1) = 6(\alpha_3 - \alpha_1 - \delta_1) - 2(\beta_1 + 4\beta_2 + \beta_3 + 2\delta_2) =: g_1 - 8\beta_2, \\ \llbracket v''' \rrbracket(1) &= \phi_2'''(1) - \phi_1'''(1) = -12(\alpha_1 - 2\alpha_2 + \alpha_3 - \delta_1) - 6(\beta_1 - \beta_3 - \delta_2) =: g_2 + 24\alpha_2. \end{aligned}$$

In order to evaluate the remaining jump terms, we represent v_1 and v_2 using the Green's function

$$v_1(x) = \int_0^1 G(x, t) (f(t) + b\phi_1''(t) - c\phi_1(t)) dt, \quad (18a)$$

$$\begin{aligned} v_2(x) &= \int_0^1 G(x - 1, t) (f(t + 1) + b\phi_2''(t + 1) - c\phi_2(t + 1) + d(\phi_1(t) - v_1(t))) dt \\ &= \int_0^1 G(x - 1, t) \left(f(t + 1) + b\phi_2''(t + 1) - c\phi_2(t + 1) + d\phi_1(t) \right. \\ &\quad \left. - d \int_0^1 G(t, s) (f(s) + b\phi_1''(s) - c\phi_1(s)) ds \right) dt. \quad (18b) \end{aligned}$$

To be more precise, we have

$$\begin{aligned} v_1(x) &= g_3(x) + \alpha_2 F_1(x) + \beta_2 F_2(x), \\ v_2(x) &= g_4(x) + \alpha_2 F_3(x) + \beta_2 F_4(x), \end{aligned}$$

where

$$\begin{aligned} g_3(x) &= \int_0^1 G(x, t) (f(t) + b(\alpha_1 \Phi_1''(t) + \beta_1 \Phi_3''(t)) - c(\alpha_1 \Phi_1(x) + \beta_1 \Phi_3(t))) dt, \\ g_4(x) &= \int_0^1 G(x-1, t) \left(f(t+1) + b(\delta_1 \Phi_1''(t) + \alpha_3 \Phi_2''(t) + \delta_2 \Phi_3''(t) + \beta_3 \Phi_4''(t)) \right. \\ &\quad \left. - c(\delta_1 \Phi_1(t) + \alpha_3 \Phi_2(t) + \delta_2 \Phi_3(t) + \beta_3 \Phi_4(t)) \right. \\ &\quad \left. + d(\alpha_1 \Phi_1(t) + \beta_1 \Phi_3(t)) - dg_3(t) \right) dt, \\ F_1(x) &= \int_0^1 G(x, t) (b\Phi_2''(t) - c\Phi_2(t)) dt, \\ F_2(x) &= \int_0^1 G(x, t) (b\Phi_4''(t) - c\Phi_4(t)) dt, \\ F_3(x) &= \int_0^1 G(x-1, t) (b\Phi_1''(t) - c\Phi_1(t) + d\Phi_2(t) - dF_1(t)) dt, \\ F_4(x) &= \int_0^1 G(x-1, t) (b\Phi_3''(t) - c\Phi_3(t) + d\Phi_4(t) - dF_2(t)) dt. \end{aligned}$$

The system we need to solve reads after rescaling

$$\begin{pmatrix} \varepsilon(F_3''(1) - F_1''(1)) & \varepsilon(F_4''(1) - F_2''(1) + 8) \\ \varepsilon^2(F_3'''(1) - F_1'''(1) - 24) & \varepsilon^2(F_4'''(1) - F_2'''(1)) \end{pmatrix} \begin{pmatrix} \alpha_2 \\ \beta_2 \end{pmatrix} = \begin{pmatrix} \varepsilon(g_1 - g_4''(1) + g_3''(1)) \\ \varepsilon^2(g_2 - g_4'''(1) + g_3'''(1)) \end{pmatrix}.$$

In the following we show, that for small ε the coefficient matrix, let us call it \mathbf{A} , is regular and its inverse is $\mathcal{O}(1)$. To do this, we look at the integrals associated with G and compute their leading terms in an ε -expansion using MAPLE. We obtain

$$\begin{aligned} \int_0^1 G_{xx}(1, t) dt &= \frac{e-1}{e+1} \varepsilon^{-1} + \mathcal{O}(1), & \int_0^1 G_{xx}(1, t)t dt &= \frac{2}{e^2-1} \varepsilon^{-1} + \mathcal{O}(1), \\ \int_0^1 G_{xx}(1, t)t^2 dt &= \frac{e^2-4e+5}{e^2-1} \varepsilon^{-1} + \mathcal{O}(1), & \int_0^1 G_{xx}(1, t)t^3 dt &= \frac{16-2e^2}{e^2-1} \varepsilon^{-1} + \mathcal{O}(1), \\ \int_0^1 G_{xx}(0, t) dt &= \frac{e-1}{e+1} \varepsilon^{-1} + \mathcal{O}(1), & \int_0^1 G_{xx}(0, t)t dt &= \frac{e^2-2e-1}{e^2-1} \varepsilon^{-1} + \mathcal{O}(1), \\ \int_0^1 G_{xx}(0, t)t^2 dt &= \frac{2e^2-6e+2}{e^2-1} \varepsilon^{-1} + \mathcal{O}(1), & \int_0^1 G_{xx}(0, t)t^3 dt &= \frac{6e^2-14e-6}{e^2-1} \varepsilon^{-1} + \mathcal{O}(1). \end{aligned}$$

Furthermore, it holds for $k \in \{0, \dots, 3\}$

$$\begin{aligned}\int_0^1 G_{xxx}(1, t)t^k dt &= \varepsilon^{-1} \left(\int_0^1 G_{xx}(1, t)t^k dt + \mathcal{O}(1) \right), \\ \int_0^1 G_{xxx}(0, t)t^k dt &= -\varepsilon^{-1} \left(\int_0^1 G_{xx}(0, t)t^k dt + \mathcal{O}(1) \right).\end{aligned}$$

In addition, we also need estimates for the double-integrals

$$\begin{aligned}\int_0^1 G_{xx}(0, t) \int_0^1 G(t, s) ds dt &= \frac{e^2 - 2e - 1}{2(1+e)^2} \varepsilon^{-1} + \mathcal{O}(1), \\ \int_0^1 G_{xx}(0, t) \int_0^1 G(t, s)s ds dt &= \frac{e^4 - 2e^3 - 2e^2 + 1}{(e^2 - 1)^2} \varepsilon^{-1} + \mathcal{O}(1), \\ \int_0^1 G_{xx}(0, t) \int_0^1 G(t, s)s^2 ds dt &= \frac{3e^4 - 10e^3 + 4e^2 + 4e - 3}{(e^2 - 1)^2} \varepsilon^{-1} + \mathcal{O}(1), \\ \int_0^1 G_{xx}(0, t) \int_0^1 G(t, s)s^3 ds dt &= \frac{12e^4 - 26e^3 - 24e^2 + 12e + 12}{(e^2 - 1)^2} \varepsilon^{-1} + \mathcal{O}(1), \\ \int_0^1 G_{xxx}(0, t) \int_0^1 G(t, s)s^k ds dt &= -\varepsilon^{-1} \left(\int_0^1 G_{xx}(0, t) \int_0^1 G(t, s)s^k ds dt + \mathcal{O}(1) \right),\end{aligned}$$

where $k \in \{0, \dots, 3\}$.

With these estimates we obtain for the entries in \mathbf{A} of the scaled system

$$\begin{aligned}\varepsilon(F_3''(1) - F_1''(1)) &= 12 \frac{3-e}{e-1} b + 6 \frac{3e^4 - 8e^3 + 1}{(e^2 - 1)^2} bd \\ &\quad + \frac{17e^2 - 26e - 39}{e^2 - 1} c - \frac{15e^4 - 22e^3 - 60e^2 + 12e + 33}{(e^2 - 1)^2} cd \\ &\quad - 2 \frac{3e^2 - 5e - 9}{e^2 - 1} d + \mathcal{O}(\varepsilon),\end{aligned}$$

$$\begin{aligned}\varepsilon(F_4''(1) - F_2''(1) + 8) &= 6 \frac{e-3}{e-1} b - 3 \frac{3e^4 - 8e^3 + 1}{(e^2 - 1)^2} bd \\ &\quad - \frac{7e^2 - 10e - 21}{e^2 - 1} c + \frac{9e^4 - 16e^3 - 28e^2 + 8e + 15}{(e^2 - 1)^2} cd \\ &\quad + 4 \frac{e^2 - 2e - 2}{e^2 - 1} d + \mathcal{O}(\varepsilon),\end{aligned}$$

$$\begin{aligned}\varepsilon^2(F_3'''(1) - F_1'''(1) - 24) &= 36 \frac{e-1}{e+1} b - 6 \frac{3e^4 - 8e^3 + 1}{(e^2 - 1)^2} bd \\ &\quad - \frac{3e-5}{e-1} c + \frac{15e^4 - 22e^3 - 60e^2 + 12e + 33}{e^2 - 1} cd \\ &\quad + 2 \frac{3e^2 - 5e - 9}{e^2 - 1} d + \mathcal{O}(\varepsilon),\end{aligned}$$

$$\begin{aligned}\varepsilon^2(F_4'''(1) - F_2'''(1)) &= -18\frac{e-1}{e+1}b + 3\frac{3e^4 - 8e^3 + 1}{e^2 - 1}bd \\ &\quad + \frac{e-1}{e+1}c - \frac{9e^4 - 16e^3 - 28e^2 + 8e + 15}{(e^2 - 1)^2}cd \\ &\quad - 4\frac{e^2 - 2e - 2}{e^2 - 1}d + \mathcal{O}(\varepsilon).\end{aligned}$$

Furthermore, for its determinant we have

$$\begin{aligned}\det(\mathbf{A}) &= -4\frac{e^4 + 4e^3 - 27e^2 + 10e + 36}{(e^2 - 1)^2}c^2 - 24\frac{e^4 - 5e^3 + 10e^2 - 11e + 3}{(e^2 - 1)^2}bd \\ &\quad - 24\frac{2e^4 - 9e^3 + 17e^2 - 11e - 3}{(e^2 - 1)^2}bc - 4\frac{5e^2 - 25e + 31}{1 - e(2)}cd \\ &\quad - 4\frac{9e^4 - 47e^3 + 59e^2 + 26e - 54}{(e^2 - 1)^2}c^2d - 6\frac{3e^4 - 12e^3 + 22e^2 - 40e + 23}{(e^2 - 1)^2}bcd + \mathcal{O}(\varepsilon).\end{aligned}$$

We therefore conclude, that \mathbf{A} is regular and $\|\mathbf{A}^{-1}\|_\infty \lesssim 1$. Thus

$$\left\| \begin{pmatrix} \alpha_2 \\ \beta_2 \end{pmatrix} \right\|_\infty \lesssim \left\| \begin{pmatrix} \varepsilon(g_1 - g_4''(1) + g_3''(1)) \\ \varepsilon^2(g_2 - g_4'''(1) + g_3'''(1)) \end{pmatrix} \right\|_\infty,$$

and for the final stability result we have to estimate the right hand side. For that let us collect the absolute values of the data:

$$\kappa := |\alpha_1| + |\alpha_3| + |\delta_1| + |\delta_2| + |\beta_1| + |\beta_3|.$$

Then the right hand side can be estimated by

$$\begin{aligned}\varepsilon|g_1| &\lesssim \varepsilon\kappa, \quad \varepsilon^2|g_2| \lesssim \varepsilon^2\kappa, \\ \|g_3\|_{L^\infty(0,1)} &\lesssim \sup_{x \in (0,1)} \int_0^1 G(x,t) dt (\|f\|_{L^\infty(0,1)} + |\alpha_1| + |\beta_1|), \\ \varepsilon|g_3''(1)| &\lesssim \varepsilon \int_0^1 |G_{xx}(1,t)| dt (\|f\|_{L^\infty(0,1)} + |\alpha_1| + |\beta_1|), \\ \varepsilon^2|g_3'''(1)| &\lesssim \varepsilon^2 \int_0^1 |G_{xxx}(1,t)| dt (\|f\|_{L^\infty(0,1)} + |\alpha_1| + |\beta_1|), \\ \varepsilon|g_4''(1)| &\lesssim \varepsilon \int_0^1 |G_{xx}(0,t)| dt \left(\|f\|_{L^\infty(1,2)} + \kappa + \|g_3\|_{L^\infty(0,1)} \right), \\ \varepsilon^2|g_4'''(1)| &\lesssim \varepsilon^2 \int_0^1 |G_{xxx}(0,t)| dt \left(\|f\|_{L^\infty(1,2)} + \kappa + \|g_3\|_{L^\infty(0,1)} \right),\end{aligned}$$

The final ingredients are the following estimates on the Green's function

$$\begin{aligned} 0 &\leq \int_0^1 G(x, t) dt \leq \int_0^1 G\left(\frac{1}{2}, t\right) dt = \frac{(e^{1/2} - 1)^2}{e + 1} + \mathcal{O}(\varepsilon), \\ \int_0^1 |G_{xx}(0, t)| dt + \int_0^1 |G_{xx}(1, t)| dt &\lesssim \varepsilon^{-1}, \\ \int_0^1 |G_{xxx}(0, t)| dt + \int_0^1 |G_{xxx}(1, t)| dt &\lesssim \varepsilon^{-2}. \end{aligned}$$

So for the unknown values at $x = 1$ we get

$$|\alpha_2| + |\beta_2| \lesssim \|f\|_{L^\infty(0,2)} + \kappa.$$

Now using $u_i = v_i + \phi_i$ and the representation formulae (18) we finally obtain

$$\|u\|_{L^\infty(0,2)} \lesssim \|f\|_{L^\infty(0,2)} + \kappa.$$

The above result is for the case $m = 1$ – first derivatives as boundary data. For $m = 2$ we can follow the same procedure. Now (7) is replaced by

$$u_1''(0) = \beta_1, u_1''(1) = \beta_2 = u_2''(1), u_2''(2) = \beta_3,$$

and α_2, β_2 are chosen such that

$$\llbracket u' \rrbracket(1) = \delta_2, \llbracket u''' \rrbracket(1) = 0.$$

To define the associated Green's function, we change the conditions (17c) to

$$G_{xx}(0, t) = 0, G_{xx}(1, t) = 0$$

and find a similar representation of G . In order to represent u by G , we again write $v_i = u_i - \phi_i$, where

$$\begin{aligned} \phi_1(x) &= \alpha_1 \Psi_1(x) + \alpha_2 \Psi_2(x) + \beta_1 \Psi_3(x) + \beta_2 \Psi_4(x), x \in (0, 1), \\ \phi_2(x) &= (\alpha_2 + \delta_1) \Psi_1(x - 1) + \alpha_3 \Psi_2(x - 1) + \beta_2 \Psi_3(x - 1) + \beta_3 \Psi_4(x - 1), x \in (1, 2) \end{aligned}$$

and $\{\Psi_k\}$ are the Hermite basis of \mathbb{P}_3 associated with the evaluation of function and second derivative values. The rest of the steps are similar and so is the result.